
Natural Computing **2:** 463–478, 2003.

Engineering signal processing in cells: Towards molecular concentration band detection

SUBHAYU BASU, DAVID KARIG and RON WEISS
Princeton University, Engineering Quadrangle, Olden Street, Princeton, NJ 08544, USA
(E-mail: {basu;dkarig;rweiss}@princeton.edu)

Abstract. We seek to couple protein-ligand interactions with synthetic gene networks in order to equip cells with the ability to process internal and environmental information in novel ways. In this paper, we propose and analyze a new genetic signal processing circuit that can be configured to detect various chemical concentration ranges of ligand molecules. These molecules freely diffuse from the environment into the cell. The circuit detects acyl-homoserine lactone ligand molecules, determines if the molecular concentration falls within two prespecified thresholds, and reports the outcome with a fluorescent protein. In the analysis of the circuit and the description of preliminary experimental results, we demonstrate how to adjust the concentration band thresholds by altering the kinetic properties of specific genetic elements, such as ribosome binding site efficiencies or dna-binding protein affinities to their operators.

Key words: cellular computation, cell-cell communications, genetic signal processing, synthetic gene networks

1. Introduction

Cells are complex information processing units that respond in highly sensitive ways to environmental and internal signals. Examples include the movement of bacteria toward higher concentrations of nutrients through the process of chemotaxis, detection of photons by retinal cells and subsequent conversion to bioelectrical nerve signals, release of fuel molecules due to hormones that signal hunger, coordinated secretion of virulence factors and degradative enzymes by bacterial cells using quorum sensing molecules, and cell differentiation based on signal gradients.

We strive to engineer cells that process internal and environmental information in novel ways by integrating protein-ligand interactions with synthetic gene networks. Applications include patterned biomaterial fabrication, embedded intelligence in materials, multi-cellular coordinated environmental sensing and effecting, and programmed therapeutics. These applications require synthesis of sophisticated and reliable cell behaviors that instruct cells to process information and make complex decisions based on factors such as extra-cellular conditions and current cell state.

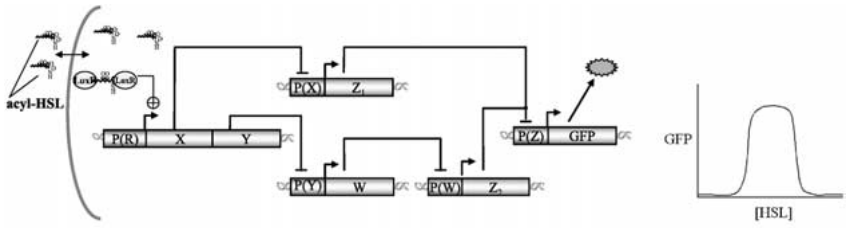

Figure 1. Gene Network for a chemical concentration band detector.

In this paper, we propose a new genetic signal processing circuit for detecting tunable ranges of chemical concentrations of ligand molecules that freely diffuse into the cell. The signal processing is performed in engineered *Escherichia Coli* hosts to detect acyl-homoserine lactone (acyl-HSL) quorum sensing molecules. The underlying mechanisms rely on ligand molecules binding to cytoplasmic proteins and the binding of cytoplasmic proteins to DNA segments that regulate the expression of other proteins. The genetic circuit consists of components that detect the level of acyl-HSL, determine if the level is within the range of two prespecified thresholds, and report the outcome with a fluorescent protein (Figure 1).

The acyl-HSL signal is produced either by naturally occurring organisms (Fuqua et al., 1994) or by bacterial hosts engineered to secrete the molecules in order to perform cell-cell communications (Weiss and Knight Jr., 2000). The acyl-HSL freely diffuses from the environment into cells and binds to the *luxR* cytoplasmic protein, enabling the protein to form a dimer. In turn, the dimer complex binds to the DNA and activates the lux P(R) promoter. The activated transcription results in the expression of regulatory proteins (X and Y) that control two series of downstream promoters. Here, DNA-binding repressor proteins X, Y, W, and Z, and their promoter counterparts are carefully chosen or engineered to have desired kinetic properties. The sub-circuit originating from the X protein determines the lower threshold of the acceptable acyl-HSL range, while the sub-circuit originating from the Y protein determines the high threshold. If the acyl-HSL chemical concentration falls within the range, the reporter green fluorescent protein (GFP) is expressed at high levels and can be detected externally. In the analysis of the circuit and the description of preliminary experimental results, we demonstrate how to adjust these thresholds by altering the kinetic properties of specific genetic elements, such as the ribosome binding site (RBS) efficiencies or the dna-binding protein affinities to their operators.

The output of the band detection circuit can be coupled to other genetic circuits and regulatory responses. This circuit is therefore useful for monitoring many protein-ligand interactions that affect gene regulation and can serve as a modular component for a variety of signal processing tasks. For

example, it can be used in cell-cell communications systems, in the detection of chemical gradients, and in synthetic cell aggregate systems that gather, process, and respond to environmental signals spanning large-scale areas.

In the remainder of the paper, we describe relevant work and background (Section 2), introduce the design of the band detection circuit (Section 3), analyze the ability to modify band thresholds (Section 4), report on preliminary experimental results that demonstrate the functioning of certain subcomponents of this circuit (Section 5), and offer conclusions and a discussion of the issues in implementing the full circuit (Section 6).

2. Background

2.1. *Quorum sensing*

Quorum sensing enables coordinated behavior among bacteria (Bassler, 1999). Specifically, acyl-homoserine lactones (acyl-HSLs) diffuse freely through cell walls and serve as intercellular communication signals. Significant accumulation of acyl-HSL results in interaction of this signal chemical with specific DNA-binding R-proteins. This bound complex then activates transcription of a certain gene or sets of genes. Synthesis of acyl-HSLs is mediated by specific I-genes. As an example, the quorum sensing system in *Vibrio fischeri*, which grows in a symbiotic relationship with sea organisms such as the Hawaiian sepiolid squid, regulates density dependent bioluminescence. In this system, the *luxI* gene codes for production of LuxI, which is responsible for synthesis of 3-oxohexanoyl-homoserine lactone (3OC6HSL). The *luxR* gene codes for the LuxR protein, which binds to accumulated 3OC6HSL to activate gene transcription. Previously, we successfully transferred this quorum sensing mechanism to *E. coli* hosts for use in engineered cell-cell communications (Weiss and Knight Jr., 2000).

2.2. *Synthetic gene networks*

Other recent projects have also experimentally demonstrated forward-engineered genetic regulatory networks that perform specific tasks in cells. Becskei's autorepressive construct (Becskei and Serrano, 2000) is a single gene that negatively regulates itself to achieve a more stable output. Gardner's toggle switch (Gardner et al., 2000) is a genetic system in which two proteins negatively regulate the synthesis of one another. This system is bistable, and sufficiently large perturbations can switch the state of the system. Elowitz's represillator (Elowitz and Leibler, 2000) is a genetic system in which three proteins in a ring negatively repress each other. This system oscillates

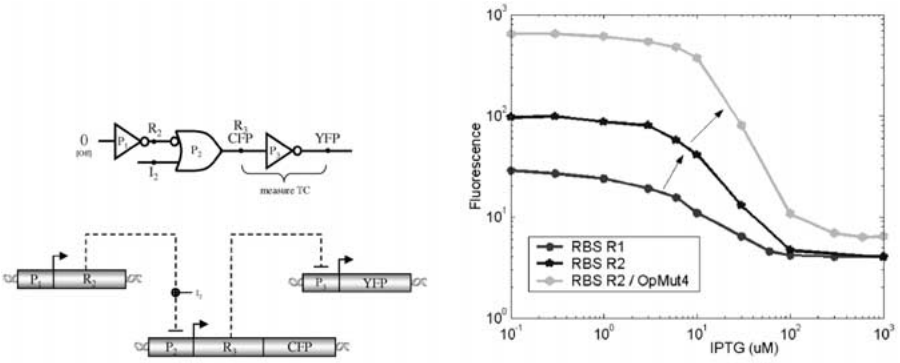

Figure 2. Genetic circuit to measure the device physics of an R_3/P_3 cellular gate: digital logic circuit and the genetic regulatory network (P_x: promoters, R_x: repressors, CFP/YFP: reporters).

between LOW and HIGH values. For the above systems, the analysis and experimental results reveal that the genetic components must be matched to achieve correct system operation, as also discussed in Weiss et al. (1999).

2.3 *Device physics of genetic circuit components*

We have previously defined genetic process engineering as a method for genetically altering system components until their device physics are properly matched. These components can then be combined into more complex circuits that achieve the desired behavior. For example, ribosome binding sites (RBS) can be mutated to alter rates of translation of mRNA into protein. We constructed genetic circuits to measure the device physics of cellular gates (Weiss and Basu, 2002), as shown in Figure 2. In one instance of this network, the R2/P2 component consists of a lacI/p(lac) gate and the R3/P3 component consists of a cI/$\lambda_{P(R)}$ gate. In this case, the level of the IPTG inducer molecule (I2) controls the level of the cI input repressor. With matching gates, the logic interconnect of this circuit should result in YFP fluorescence intensities that are inversely correlated with the IPTG input levels. The lowest curve in Figure 2 (RBS R1) shows the transfer curve of a cI/$\lambda_{P(R)}$ inverter prior to genetic process engineering. The transfer curve relates IPTG input concentrations to the median fluorescence of cells grown in a culture at these IPTG concentrations. The cells were grown for several hours in log phase until protein expression reached a steady state. The unmodified cI/$\lambda_{P(R)}$ circuit responds weakly to variations in the IPTG inducer levels.

Genetic process engineering was used to modify the cI/$\lambda_{P(R)}$ inverter to obtain improved behavioral characteristics. Ribosome Binding Site (RBS) sequences significantly control the rate of translation from messenger RNA

(mRNA) molecules to the proteins for which they code. We replaced the original highly efficient RBS of cI with a weaker RBS site by site-directed mutagenesis and were able to noticeably improve the response of the circuit (Figure 2, RBS R2). In further genetic process engineering (Figure 2, RBS R2/OpMut4), a one base pair mutation to the cI operator site of $\lambda_{P(R)}$ yields a circuit with an improved inverse sigmoidal response to the IPTG signal.

The signal processing circuits described in Section 3 are assembled by combining multiple genetic components with matching characteristics into compound circuits. To effectively synthesize these compound circuits, the device physics of circuit components can be engineered using site-directed mutagenesis and molecular evolution techniques. Note that the genetic constructs for digital logic inverters described in this section are also used for the low threshold component of the band detection circuit.

3. Design of chemical concentration band detection

The proposed construction for a chemical concentration band detector circuit, shown in Figure 1, expresses high levels of the reporter gene (GFP) only when the concentration of the acyl-HSL signal is within a specific range. The genetic circuit consists of three subcircuits: a low threshold detector, a high threshold detector, and a negating combiner.

The series of transcriptional regulators that originates from repressor protein X determines the low threshold. When acyl-HSL binds the R-protein, the molecular complex activates transcription of protein X. In turn, high concentrations of protein X repress P(X) promoter production of protein Z (labeled as Z_1 because Z can also be expressed from the P(W) promoter). Similarly, the series of transcriptional regulators that originates from repressor protein Y determines the high threshold by regulating expression of Z from P(W) (labeled as Z_2). Therefore, Z is expressed from P(X) when acyl-HSL is below the low threshold and from P(W) when acyl-HSL is above the high threshold. This combined production of protein Z from P(X) and P(W) determines the chemical concentration range for detection. Finally, the repression of promoter P(Z) by protein Z causes GFP expression to be high only when the acyl-HSL concentration falls within the prespecified range.

3.1. *Biochemical model*

Table 1 shows the chemical reactions used to model the production of proteins *X* and *Y* from Lux_{PR} in response to incoming acyl-HSL. RNA polymerase (RNA_p) transcribes messenger RNA (mRNA) from DNA, and ribosomal RNA (rRNA) translates mRNA into protein.[1] Through transcription and

Table 1. Chemical reactions that model expression of proteins X and Y in response to incoming acyl-HSL (AHL)

$Lux_{\mathrm{PL}} + \mathrm{RNA}_p$	$\xrightarrow[\text{transcribe}]{k_{\text{xscribe(luxR)}}}$	$Lux_{\mathrm{PL}} + \mathrm{RNA}_p + \mathrm{mRNA}_{\mathrm{luxR}}$	(1)
$\mathrm{mRNA}_{\mathrm{luxR}}$	$\xrightarrow[\text{decay}]{k_{\text{dec(mrna)}}}$		(2)
$\mathrm{mRNA}_{\mathrm{luxR}} + \mathrm{rRNA}$	$\xrightarrow[\text{translate}]{k_{\text{xlate(luxR)}}}$	$\mathrm{mRNA}_{\mathrm{luxR}} + \mathrm{rRNA} + \mathrm{LuxR}$	(3)
LuxR	$\xrightarrow[\text{decay}]{k_{\text{dec(luxR)}}}$		(4)
$2\ \mathrm{LuxR} + 2\ \mathrm{AHL}$	$\xrightarrow[\text{associate}]{k_{\text{assoc(AHL)}}}$	$\mathrm{LuxR}_2\mathrm{AHL}_2$	(5)
$\mathrm{LuxR}_2\mathrm{AHL}_2$	$\xrightarrow[\text{dissociate}]{k_{\text{dis(AHL)}}}$	$2\ \mathrm{LuxR} + 2\ \mathrm{AHL}$	(6)
$\mathrm{LuxR}_2\mathrm{AHL}_2$	$\xrightarrow[\text{decay}]{k_{\text{dec}(\mathrm{R_2HL_2})}}$		(7)
$\mathrm{LuxR}_2\mathrm{AHL}_2 + \mathrm{Lux}_{\mathrm{PR}}$	$\xrightarrow[\text{activate}]{k_{\text{activ}(\mathrm{R_2HL_2})}}$	$\mathrm{Lux}_{\mathrm{PR}}\mathrm{R}_2\mathrm{HL}_2$	(8)
$\mathrm{Lux}_{\mathrm{PR}}\mathrm{R}_2\mathrm{HL}_2$	$\xrightarrow[\text{dissociate}]{k_{\text{dis}(\mathrm{luxR_2})}}$	$\mathrm{LuxR}_2\mathrm{AHL}_2 + \mathrm{Lux}_{\mathrm{PR}}$	(9)
$\mathrm{Lux}_{\mathrm{PR}}\mathrm{R}_2\mathrm{HL}_2$	$\xrightarrow[\text{decay}]{k_{\text{dec}(\mathrm{L_{PR}RH_2})}}$	$\mathrm{Lux}_{\mathrm{PR}}$	(10)
$\mathrm{Lux}_{\mathrm{PR}}\mathrm{R}_2\mathrm{HL}_2 + \mathrm{RNA}_p$	$\xrightarrow[\text{transcribe}]{k_{\text{xscribe(XY)}}}$	$\mathrm{Lux}_{\mathrm{PR}}\mathrm{R}_2\mathrm{HL}_2 + \mathrm{RNA}_p + \mathrm{mRNA}_{\mathrm{XY}}$	(11)
$\mathrm{mRNA}_{\mathrm{XY}}$	$\xrightarrow[\text{decay}]{k_{\text{dec(mrna)}}}$		(12)
$\mathrm{mRNA}_{\mathrm{XY}} + \mathrm{rRNA}$	$\xrightarrow[\text{translate}]{k_{\text{xlate(X)}}}$	$\mathrm{mRNA}_{\mathrm{XY}} + \mathrm{rRNA} + \mathrm{X}$	(13)
$\mathrm{mRNA}_{\mathrm{XY}} + \mathrm{rRNA}$	$\xrightarrow[\text{translate}]{k_{\text{xlate(Y)}}}$	$\mathrm{mRNA}_{\mathrm{XY}} + \mathrm{rRNA} + \mathrm{Y}$	(14)

translation, LuxR is constitutively expressed from $\mathrm{Lux}_{\mathrm{PL}}$ (reactions 1-4). The $active$ form of $\mathrm{Lux}_{\mathrm{R}}$ is produced by the binding of acyl-HSL (AHL) and LuxR to form $\mathrm{LuxR}_2\mathrm{AHL}_2$ (reaction 5). The $\mathrm{Lux}_{\mathrm{PR}}$ promoter is typically *inactive*. Activation of the $\mathrm{Lux}_{\mathrm{PR}}$ promoter by $\mathrm{LuxR}_2\mathrm{AHL}_2$ binding (reaction 8) results in expression of X and Y (reaction 11–14). $mRNA_{\mathrm{luxR}}$ is the gene transcript coding for LuxR and $mRNA_{\mathrm{XY}}$ is the gene transcript coding for both X and Y.

Table 2 presents the biochemical model for a repression component of the band detector circuit. These reactions model the repression of Z_1 by X, W by Y, Z_2 by W, and GFP by Z. The particular repression model reflects the characteristics of the lambda CI repressor operating on the lambda $\mathrm{O_R}1$ and $\mathrm{O_R}2$ operators, which is representative of the repressors used in our system. In a repressor component, a repressor protein A is the input, and protein B is the

Table 2. Chemical reactions that implement a typical repressor component. A is the input protein and B the output.

$$A + A \xrightarrow[\text{dimerization}]{k_{\text{dim(a)}}} A_2 \quad (15)$$

$$A_2 \xrightarrow[\text{single}]{k_{\text{sngl(a)}}} A + A \quad (16)$$

$$B + B \xrightarrow[\text{dimerization}]{k_{\text{dim(b)}}} B_2 \quad (17)$$

$$B_2 \xrightarrow[\text{single}]{k_{\text{sngl(b)}}} B + B \quad (18)$$

$$P_B + A_2 \xrightarrow[\text{repress 1}]{k_{\text{rprs(a2)}}} P_B A_2 \quad (19)$$

$$P_B A_2 \xrightarrow[\text{dissociation}]{k_{\text{dis(a2)}}} P_B + A_2 \quad (20)$$

$$P_B A_2 + A_2 \xrightarrow[\text{repress 2}]{k_{\text{rprs(a4)}}} P_B A_4 \quad (21)$$

$$P_B A_4 \xrightarrow[\text{dissociation}]{k_{\text{dis(a4)}}} P_B A_2 + A_2 \quad (22)$$

$$A \xrightarrow[\text{decay}]{k_{\text{dec(a)}}} \quad (23)$$

$$A_2 \xrightarrow[\text{decay}]{k_{\text{dec(a2)}}} \quad (24)$$

$$B \xrightarrow[\text{decay}]{k_{\text{dec(b)}}} \quad (25)$$

$$B_2 \xrightarrow[\text{decay}]{k_{\text{dec(b2)}}} \quad (26)$$

$$P_B A_2 \xrightarrow[\text{decay}]{k_{\text{dec(pba2)}}} P_B \quad (27)$$

$$P_B A_4 \xrightarrow[\text{decay}]{k_{\text{dec(pba4)}}} P_B A_2 \quad (28)$$

$$mRNA_B \xrightarrow[\text{decay}]{k_{\text{dec(mrna)}}} \quad (29)$$

$$P_B + RNA_p \xrightarrow[\text{transcribe}]{k_{\text{xscribe(b)}}} P_B + RNA_p + mRNA_B \quad (30)$$

$$mRNA_B + rRNA \xrightarrow[\text{translate}]{k_{\text{xlate(b)}}} mRNA_B + rRNA + B \quad (31)$$

output. P_B denotes the concentration of the *active* form of the promoter for B. As opposed to the Lux_{PR} promoter above, promoter P_B is active only when its associated operator is *unbound* by a repressor. A_2 and B_2 denote the dimeric forms of A and B respectively, and $P_B A_2$ and $P_B A_4$ represent the repressed (i.e., inactive) forms of the promoter. $mRNA_B$ is the gene transcript coding for B. Important aspects of the model include dimerization of the protein (reactions 15–18), cooperative binding (reactions 19–22), transcription and translation (reactions 30, 31), and degradation of proteins and mRNA (reactions 23–29). The kinetic constants used in the simulations are listed in Weiss et al. (1999) and are based on the literature describing the phage λ promoter P_R and repressor (cI) mechanism in Ptashne (1986) and Hendrix (1983), in addition to educated guesses.

3.2. *Simulation of band detection*

Figure 3(a) shows a simulation of the steady state response of P(X) transcription of protein Z with respect to varying HSL concentrations. The simulations illustrate the average messenger RNA (mRNA) levels for X and Z_1 in a cell

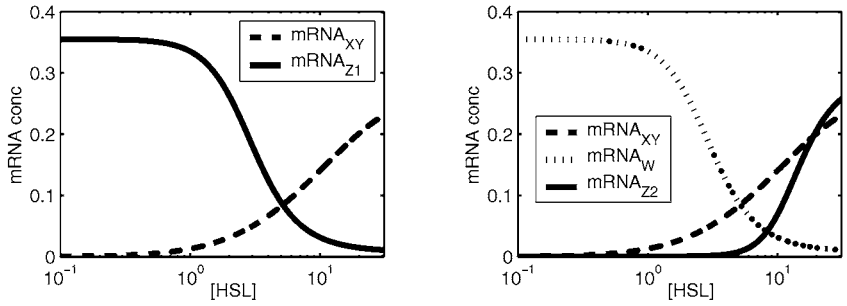

(a) low threshold (b) high threshold

Figure 3. Low threshold and high threshold sub-circuits.

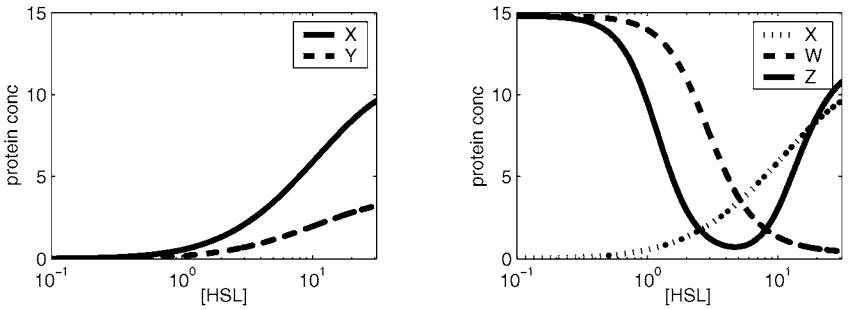

(a) X versus Y expression (b) X and W determine total Z

Figure 4. Determinants of the band detector.

that contains the band detect circuit, with all units denoting μmolar concentrations. As shown, $mRNA_{Z1}$ is HIGH only if the level of HSL is LOW. Notice that P(R) is multi-cistronic, coding for both X and Y that are expressed from $mRNA_{XY}$. However, the translation rates of X and Y are different due to the fact that the carefully chosen RBS efficiencies for the respective proteins differ. In Weiss and Basu (2002) and Section 2, we demonstrate the ability to quantitatively modify the transfer curve characteristics of genetic components by using a variety of RBSs.

The second subcircuit, which determines the high threshold, consists of transcriptional regulators that originate from protein Y. Figure 3(b) shows the steady state relationship between HSL input levels and mRNA levels for XY, W, and Z_2. The RBS for Y is weaker than the RBS for X. Therefore Y is produced at lower rates than X for any given level of HSL (Figure 4(a)). As a result of the lower rate of protein Y expression, protein W is still highly expressed in response to HIGH HSL levels when P(X) is already inactivated. This allows P(W) to act as the high threshold detector by transcribing Z only when the HSL input is above a certain level.

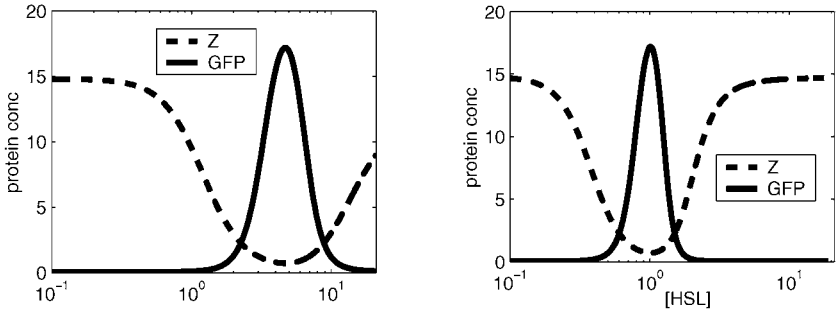

(a) original band detector (b) modified band detector

Figure 5. Different band detectors from negating Z.

The last subcircuit combines the output of the two preceding subcircuits and negates their total product to produce the band detector. Figure 4(b) illustrates how the level of Z in the cell is determined by both X and W. Logically, Z is HIGH when either X or W is LOW (Z = X NAND W). The output protein Z functions as a band-reject circuit. Finally, Figure 5(a) shows how the combined level of Z from transcription of both P(X) and P(W) represses the final GFP output, resulting in a band detector. By tuning reaction kinetics such as RBS efficiencies, protein decay rates, and protein-operator affinities, this synthetic gene network can be configured to respond to different signal ranges. For example, Figure 5(b) shows how to modify the band detector to accept a lower threshold by choosing ribosome binding sites for proteins X and Y that are three-fold more efficient.

The simulation results described here were obtained by integrating ordinary differential equations that describe the biochemical reactions of the band detector circuit. The simulations demonstrate the qualitative effects of modifying genetic components in the forward engineering of synthetic gene networks. In the graphs, the nonlinear response of the components is due to repressor protein dimerization and the existence of multiple operator sites. We have used both of these common genetic regulatory motifs in previous experiments (Weiss and Basu, 2002). The next section analyzes the ability to change band thresholds by modifying various kinetic parameters of the circuit components.

4. Forward engineering of band characteristics

This section examines forward engineering of band characteristics through the modification of two genetic regulatory elements: RBS's and repressor/operator affinities. Two key characterizations of a band detect circuit are the

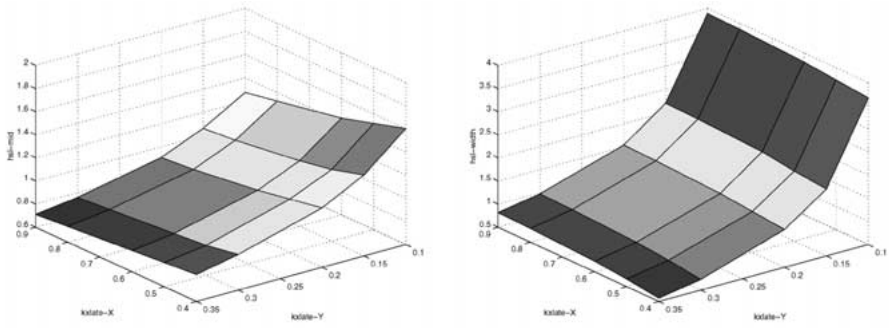

(a) HSL midpoint of band detector (b) HSL width of band detector

Figure 6. Impact of modifying X and Y RBS efficiencies on band midpoint and width.

midpoint of its detection range and the width of this range. The width is defined as the distance between the low and high cutoff points. The cutoff point is the HSL level at which the output of the band detector switches between what a downstream circuit considers HIGH or detectable and what it considers LOW or undetectable. For the analysis below, we define the cutoffs as the HSL input levels at which the output GFP concentration is 0.3 μM. We assume that GFP concentrations above this threshold can be reliably detected by flow cytometry.

Figure 6 depicts the effects of simultaneously changing the RBS efficiencies of X (kxlate_X) and Y (kxlate_Y) on the midpoint and width of the band detector. The x and y axes represent the various RBS efficiencies, while the z axis depicts the HSL midpoint and HSL band width. As the RBS efficiency of protein X increases, a given HSL level results in additional translation of protein X. Thus, less mRNA_{Z1} is transcribed, and the low threshold component of the Z protein curve shifts left. This shift increases the band width and moves the midpoint left. As the RBS efficiency for Y increases, the high threshold component of the Z protein curve also shifts left, causing the band width to decrease and the midpoint to move left.

The impact of simultaneously altering the binding affinities of the X_2 and Y_2 dimer proteins to their respective promoters is illustrated in Figure 7. If an X_2 dimer binds more readily to the promoter responsible for transcription of mRNA_{Z1}, the low threshold component of the Z protein curve shifts left. This shift in turn causes the width of the band to increase and moves the midpoint to the left. As the strength of Y repression increases, the high threshold component of the Z protein curve shifts left, decreasing the band width and moving the midpoint left.

A recurring trend in the analysis here is that changes in the RBS efficiency and the repression strength of Y have a greater impact on the shape of the

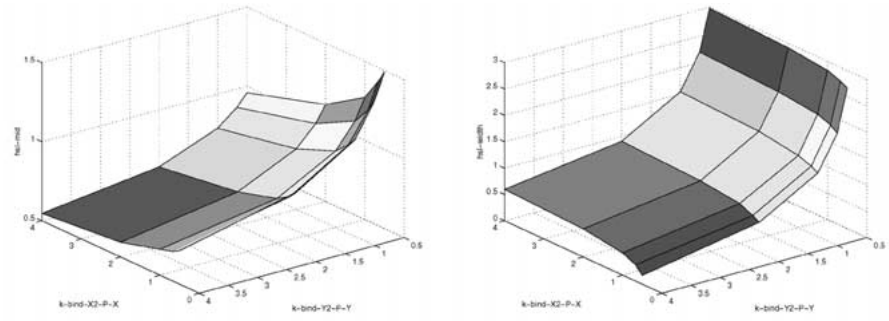

(a) HSL mid point for band detector (b) HSL width for band detector

Figure 7. Impact of modifying X and Y protein/operator binding affinities.

band than comparable changes in the RBS efficiency and repressive strength of X. One reason that the constants associated with Y have greater impact is that Y influences the Z protein curve through an additional gain stage resulting from the W repressor. Simulations reveal that if the binding constant of W to its promoter and the RBS efficiency of W are reduced, the impact of Y on the HSL midpoint and band width are also reduced (graphs not shown). Another reason for the discrepancy is that Y controls Z values that correspond to a higher range of the HSL input signal than the Z values controlled by X.

5. Preliminary experimental results

In this section, we describe preliminary experimental results that demonstrate the functioning of certain subcircuits for performing band detection. Section 2 describes previous results of a low threshold subcircuit tunable by modifications of ribosome binding site efficiencies and repressor/operator affinities. In the next two sections, we present new experimental data for detecting a high threshold and for responding to acyl-HSL signals.

5.1. *Implementation of high threshold detection*

To detect molecular concentrations above specific thresholds, we constructed the two plasmids in Figure 8 using standard DNA cloning techniques (Ausubel et al., 1999; Sambrook et al., 1989). The pCMB-2 plasmid contains an ampicillin resistance gene and a medium copy number origin of replication (ColE1 ORI). It also has a tet repressor (TetR) gene coding sequence that is transcribed from the ampicillin p(bla) promoter. The *tetR* regulates the P(LtetO-1) promoter on the pCMB-100 plasmid (kanamycin resistance, p15A medium copy number origin of replication). The lac repressor (*lacI*), which

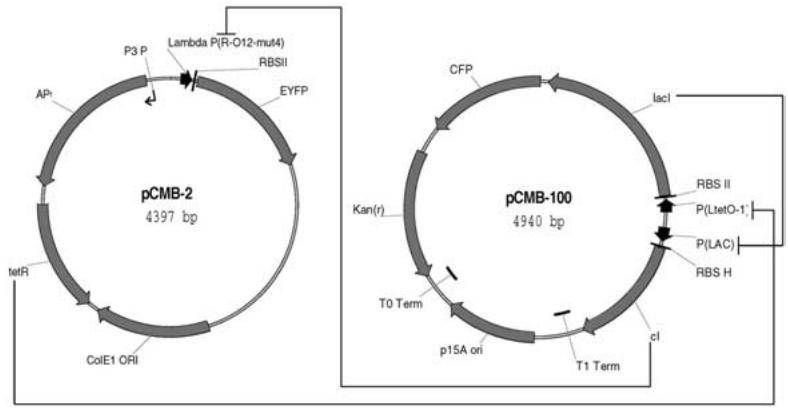

Figure 8. pCMB-2 and pCMB-100.

corresponds to protein Y in Figure 1, and cyan fluorescent protein (CFP) from Clontech are transcribed from the P(LtetO-1) promoter. CFP reports the *lacI* levels. When the anhydrotetracycline (aTc) inducer molecule is introduced into the cell, it binds to TetR and prevents TetR from repressing P(LtetO-1). The aTc inducer molecule functions as the external input to the high threshold circuit component.

The *lacI* protein represses P(lac) and regulates the expression of *cI*, which corresponds to protein W in Figure 1 and is the λ repressor protein (Ptashne, 1986). *cI* is a highly efficient repressor that exhibits dimerization and cooperative binding to its operator. Finally, the $\lambda_{p(R-O12-mut4)}$ promoter (Weiss and Basu, 2002) on pCMB-2 is repressed by *cI* and regulates the expression of the enhanced yellow fluorescent protein (EYFP) output of the circuit which reflects the level of protein Z in Figure 1. Therefore, the relationship between the aTc input and EYFP output describes the behavior of the high threshold component.

To experiment with this circuit, we prepared twelve tubes each of 2 ml LB ampicillin/kanamycin solution with different concentrations of aTc. We transformed *E. coli* STBL2 cells from Invitrogen with both the pCMB-2 and pCMB-100 plasmids and picked a single colony into fresh media. The culture was distributed to the twelve different tubes that were shaken at 250 RPM and @37 °C for approximately 6 hours until they reached an optical density at 600 nm of approximately 0.3. The cells were washed with 0.22 μm filter-sterilized phosphate buffered saline (PBS) twice, and the fluorescence levels of the cells were measured using Fluorescence-Activated Cell Sorting (FACS) (Shapiro, 1995) on a FACSVantage flow cytometer. The machine has two argon excitation lasers, one set at 458 nm with an emissions filter of 485/22 nm for detecting CFP, and the other laser set at 514 nm excitation with

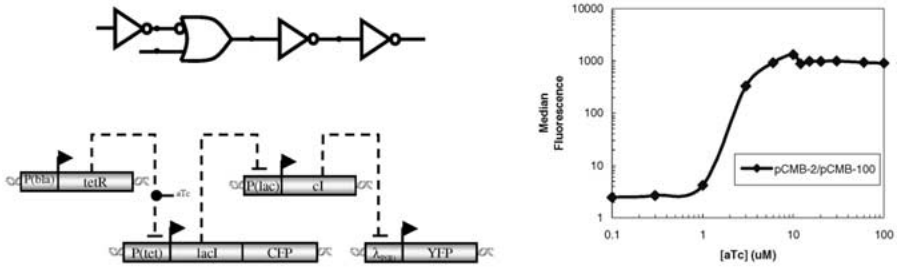

Figure 9. High threshold component of the band detector: circuit design and experimental results.

an emissions filter of 575/26 nm for detecting EYFP. Filters were obtained from Omega Optical.

Figure 9 shows the median fluorescence level for the cell populations grown with different aTc inducer concentrations. The EYFP exhibits a strong sigmoidal relationship to the aTc input levels with a sharp transition from LOW to HIGH output. The results in Figures 9 and 2 demonstrate components that respond specifically to signals bound by low or high thresholds. However, these subcircuits currently respond to either IPTG or aTc inputs, and their behavior cannot be compared directly. To synthesize an operational band detector, it is likely that we will need to reduce the strength of the response for the high threshold. The next section describes a circuit that responds to acyl-HSL levels.

5.2. *Implementation of an acyl-hsl detect circuit*

We previously constructed plasmids for performing cell-cell communications (Weiss and Knight Jr., 2000). These plasmids are pSND-1, pPROLAR.A122, and pRCV-3. The pSND-1 plasmid, which has a p(Lac) promoter and a *luxI* gene sequence, is used to produce acyl-HSL. This plasmid has a ColE1 replication origin and ampicillin resistance. The *luxI* gene encodes an acyl-homoserine lactone synthesase that uses highly available metabolic precursors found within most gram negative prokaryotic bacteria (acyl-ACP from the fatty acid metabolic cycle, and S-adenosylmethionine from the methionine pathway) to synthesize N-(3-oxohexanoyl)-3-amino-dihydro-2-(3H)-furanone, or 3OC6HSL. The pPROLAR.A122 plasmid is used as a negative control and contains only a p15A origin of replication and kanamycin resistance. The pRCV-3 plasmid, which contains a luxP(R) promoter followed by a GFP(LVA) coding sequence from Clontech, and a luxP(L) promoter followed by a *luxR* coding sequence. pRCV-3 is used for quantifying the response to acyl-HSL signals.

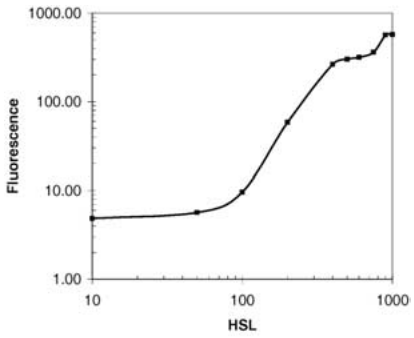

Figure 10. Median fluorescence of cell cultures with different levels of HSL.

The results in Weiss and Knight Jr. (2000) report on the relationship between acyl-HSL levels and the corresponding GFP fluorescence induced in pRCV-3. For high levels of an acyl-HSL extract, the level of fluorescence was observed to decrease. The decrease in fluorescence was likely due to the toxicity of the acyl-HSL extract. For this paper, we modified the experimental protocol in order to avoid using the acyl-HSL extract. Cells with pSND-1 plasmids were first grown @37 °C to an optical density of 0.3. These plasmids produced acyl-HSL, which diffused freely through the cell membrane. The cells were centrifuged at 6000 g, and the HSL-containing supernatant was extracted. At the same time, different cells with pPROLAR.A122 were grown @37 °C to an optical density of 0.3, and the supernatant was extracted following centrifugation at 6000 g. The pPROLAR.A122 supernatant was used to dilute the HSL-containing supernatant to various concentrations. This was done to keep the nutrient concentration the same in all of the tubes while varying the HSL concentrations. Each dilution was aliquotted into a tube containing 1 ml of fresh LB with ampicillin and kanamycin. We also added ampicillin and kanamycin as appropriate to keep the final concentrations of these antibiotics the same as in the original 1ml LB/ampicillin/kanamycin solution.

A single colony of cells transformed with both the pRCV-3 and the pPROLAR.A122 plasmids was selected and grown in the separate tubes @37 °C until the cultures reached optical density of approximately 0.3. Next, the cells were washed and resuspended in 0.22 μm filter-sterilized PBS, and the fluorescence of the cell population was measured using a FACScan flow cytometer with an argon laser excitation at 488nm and emissions filter of 530/30 nm. Figure 10 shows the median fluorescence of each of the different samples that exhibits a direct sigmoidal relationship to increasing HSL concentrations. The cells did not exhibit any decrease in fluorescence as the HSL concentration was increased.

6. Conclusions

In this paper, we propose to couple protein-ligand interactions with synthetic gene networks for detecting molecular signal concentration bands. The analysis of the circuit demonstrates several factors that can help forward-engineer this circuit to acquire different thresholds for the band detection. We also presented preliminary experimental results of the functioning of the low threshold component, the high threshold component, and the ability to respond to acyl-HSL signals.

In the effort to build the complete version of this circuit, great emphasis will be placed on the quantitative characterization of the components, including the study of cell population statistics. To arrive at components with the appropriate device physics, we plan to employ site-directed mutagenesis and molecular evolution techniques. The mechanisms employed and lessons learned in building this particular circuit are likely to be beneficial for the broader goal of building a variety of novel signal processing circuits in cells.

Note

[1] In the simulations here, the concentrations of RNA_p and rRNA are fixed.

References

Ausubel FM, Brent R, Kingston RE, Moore DD, Seidman JG, Smith JA and Struhl K (1999) Short Protocols in Molecular Biology. Wiley

Bassler BL (1999) How bacteria talk to each other: Regulation of gene expression by quorum sensing. Current Opinion in Microbiology 2: 582–587

Becskei A and Serrano L (2000) Engineering stability in gene networks by autoregulation. Nature 405: 590–593

Elowitz M and Leibler S (2000) A synthetic oscillatory network of transcriptional regulators. Nature 403: 335–338

Fuqua WC, Winans S and Greenberg EP (1994) Quorum sensing in bacteria: The LuxR-LuxI family of cell density-responsive transcriptional regulators. J. Bacteriol 176: 269–275

Gardner T, Cantor R and Collins J (2000) Construction of a genetic toggle switch in *Escherichia coli*. Nature 403: 339–342

Hendrix RW (1983) *Lambda II*. Cold Spring Harbor Press, Cold Spring Harbor, New York

Ptashne M (1986) A Genetic Switch: Phage lambda and Higher Organisms, 2nd edition. Cell Press and Blackwell Scientific Publications, Cambridge, MA

Sambrook J, Fritsch EF and Maniatis T (1989) Molecular Cloning: A Laboratory Manual. Cold Spring Harbor Laboratory Press, Plainview, NY

Shapiro HM (1995) Practical Flow Cytometry, 3rd edition. Wiley-Liss, New York, NY

Weiss R and Basu S (2002) The device physics of cellular logic gates. In: NSC-1: The First Workshop of Non-Silicon Computing. Boston, Massachusetts

Weiss R, Homsy G and Knight TF Jr. (1999) Toward in-vivo digital circuits. In: Dimacs Workshop on Evolution as Computation. Princeton, NJ

Weiss R and Knight TF Jr. (2000) Engineered communications for microbial robotics. In: DNA6: Sixth International Workshop on DNA-Based Computers, DNA2000, pp. 1–16. Leiden, The Netherlands, Springer-Verlag